International Journal of Science and Research Archive

eISSN: 2582-8185

Cross Ref DOI: 10.30574/ijsra

Journal homepage: https://ijsra.net/

(RESEARCH ARTICLE)

Check for updates

Evaluating denoising performances of basic filters in the detection of microcalcifications on mammogram images

Franca Oyiwoja Okoh * and John Actor Ocheje

Department of Pure and Applied Physics, Federal University Wukari, PMB 1020 Wukari-Taraba State, Nigeria.

International Journal of Science and Research Archive, 2023, 09(02), 201–210

Publication history: Received on 01 June 2023; revised on 09 July 2023; accepted on 12 July 2023

Article DOI: https://doi.org/10.30574/ijsra.2023.9.2.0544

Abstract

This research evaluates the denoising abilities of some image-processing filters used in facilitating the early detection of microcalcifications in breast tissues. The mean, median and Gaussian filters were employed to denoise mammogram images of microcalcification breast phantoms of various densities. The performances of the filters were assessed by evaluating the mean squared error (MSE), peak signal-to-noise ratio (PSNR), and signal-to-noise ratio (SNR). All experiments were carried out on MATLAB R2020a platform. The results revealed that the Gaussian filter recorded optimal performance in denoising images with all 3 types of added noises compared to the mean and median filters. The PSNR value of the heterogeneous phantom (PVAL/H) was superior to those of the less dense (PVAL/E), dense (PVAL), and extremely dense (PVAL/G) phantoms for all the tested filters. The results of this work agree with the high contrast recorded by the original image of PVAL/H.

Keywords: Breast cancer; Mean filter; Median filter; Gaussian filter; MSE; SNR; PSNR

1. Introduction

Breast cancer is the second leading cause of cancer death among women worldwide (Dubey, Hanmandlu and Gupta, 2010). There have been a lot of consistent efforts to tackle this disease. The presence of microcalcifications (MC) could be an early sign of breast cancer (Arvelos *et al.*, 2017). Microcalcifications are small-scale deposits of calcium found inside the breast tissue. They can be present in any part of the breast and most women will have a few on their mammograms at some point in time, especially after menopause (Oliver *et al.*, 2012). Most MC are not palpable and may not be decerned in the course of clinical or self-examination of the breast. Nevertheless, mammography helps to detect MC long before they become palpable lumps (Oliver *et al.*, 2012; O'Grady and Morgan, 2018).

Generally, early detection and subsequent treatment is key in breast cancer management. However, in some cases, it may be difficult to detect malignant lesions due to their similar appearance to glandular tissues of the breast, especially in young women with dense breast tissues. Mammography is presently the gold standard modality for detecting breast cancer in its early stage. It functions pretty well in postmenopausal women and is affordable (Kabir, Okoh and Mohd Yusof, 2021). Although like most medical procedures, mammography is not perfect, it can detect approximately 85% of breast cancers in women who do not present any symptoms (Ponraj and Jenifer, 2011).

Unlike other clinical images, mammogram images are challenging to interpret. This is because dense breast tissues appear whitish like MCs on mammograms. This resulting similarity that exists between lesions and normal breast tissue makes pre-processing a vital tool in enhancing the visibility of MCs on mammograms. This research will assess the performance of three different filters namely, mean filter, median filter, and Gaussian filter based on MSE, SNR and PSNR in denoising mammogram images of breast phantoms to enhance the visibility of MCs.

* Corresponding author: Franca Oyiwoja Okoh

2. Material and methods

Four mammogram images of polyvinyl alcohol (PVAL) based breast phantoms with embedded microcalcifications were used in this work. The phantoms were produced in our previous research (Kabir, Okoh and Mohd Yusof, 2021; Okoh *et al.*, 2022) to mimic various densities of the female breast tissue based on the BIRADS (Breast Imaging Reporting and Data System) classification. Images of the phantoms were acquired using full field digital mammography (FFDM) at 28kVp. Table 1 shows the composition of each phantom

Table 1 Breast phantom composition and BIRADS category represented

S/no	Composition of phantom	Nomenclature	BIRADS category[a]
1	10% PVAL + ethanol solution	PVAL/E	B (less dense)
2	10% PVAL (water based)	PVAL	C (dense)
3	10% PVAL + Graphite powder	PVAL/G	D (extremely dense)
4	PVAL+PVAL+PVAL/G	PVAL/H	Heterogenous

(American College of Radiology, 2013)[a]

2.1. Pre-processing

Image pre-processing is seen as the main stage in image processing procedure. The greatest objective of image pre-processing is to enhance image quality by suppressing undesired distortions or improve some image attributes which are vital for onward processing of the image. Three different filters namely mean filter, median filter, and Gaussian filter were used in this research to denoise mammogram images of breast phantoms. All 3 filters were used to remove three types of noise viz: salt and pepper, Gaussian, and speckle noise. 10% noise density was added to the mammogram images before applying filters.

(a) Mean (average) filter

The average filtering process evaluates the mean of the corrupted image g(x, y) in the area $s_{xy.}$ Where $\hat{f}(x, y)$ represents the average calculated using the pixels in regions $s_{xy.}$ sub image window of size mn. The equation for the mean filter is given by equation 1.

$$\hat{f}(x, y) = \frac{1}{mn} \sum_{(s,t)\in s_{x,y}} g(s, t) \quad \ldots . (1)$$

(b) Median filter

The median filter is a nonlinear statistical filter that replaces the current pixel value with the median value of pixels in the neighbouring region (Ramani, Vanitha and Valarmathy, 2013). Equation 2 represents the mathematical expression for the median filter.

$$Y_i = \{W_i\} = med\{X_i + r : r \in W\} \ldots \ldots \ldots (2)$$

Where $[W_i]_r r = 1, \ldots 2N + 1$, the ith order statistics of the samples inside the window W_i is $[W_1]_1 < [W_2]_2 < \cdots [W_i]_{2N+1}$

(c) Gaussian filter

The main function of Gaussian filter is to minimize the low and high signals from distortion (Kshema, George and Dhas, 2017). The Gaussian elimination algorithm was based on the mathematical description in Equation 3.

$$G(x, y) = \frac{1}{2\pi\sigma^2} e^{-(x^2+y^2)/(2\sigma^2)} \ldots . (2)$$

Where x is the distance from the origin in the horizontal axis, y is the distance from the origin in the vertical axis and σ is the standard deviation of the Gaussian distribution.

All filtered images were further postprocessed using adaptive thresholding technique.

2.2. Measurement of filter performance

Three image quality metrics (IQM) were employed in evaluating the performance of the mean, median and Gaussian filters used in this work. They include the mean square error (MSE), signal to noise ratio (SNR), and peak signal to noise ratio (PSNR). These image quality parameters are accepted, straightforward and not difficult to calculate (Zhang *et al.*, 2012; Isa *et al.*, 2015).

The mathematical expressions for MSE, SNR and PSNR can be seen in equation 4, 5 and 6 respectively.

$$MSE = \frac{1}{M.N}\sum_{m=0}^{m=1}\sum_{n=0}^{n=1}\left[I(m,n) - \hat{I}(m,n)\right]^2 \ldots\ldots\ldots(4)$$

Where I is the input image, $\hat{I}$ is the estimation of the input image acquired from a noisy one, M and N are the number of rows and columns in the input and output images respectively.

$$PSNR = 10log_{10}\frac{255^2}{MSE} \ldots\ldots..(5)$$

$$SNR = \frac{P_{signal}}{P_{noise}} \ldots\ldots\ldots.(6)$$

where P is average power.

3. Results and discussion

Figure 1 (a) – (d) to Figure 3 (a) – (d) show the original mammogram images of the 4 breast phantoms used in this research, i.e PVAL/E, PVAL, PVAL/G and PVAL/H and the quality of images obtained after application of image processing techniques based on mean filter, median filter, and Gaussian filter

3.1. Mean filter

Figure 1 (a) - (d) show the images of PVAL/E, PVAL, PVAL/G and PVAL/H enhanced through the application of mean filter. The salt & pepper and speckle noise depicted better enhancement with this filter. The results show that all 6 embedded MCs were visible in the original binary images and post processed images of PVAL/E and PVAL/H. Only 4 and 2 MCs were visible on the PVAL and PVAL/G images respectively. The mean filter showed better noise removal ability for speckle noise compared to salt & pepper and Gaussian noise.

(a) PVAL/E

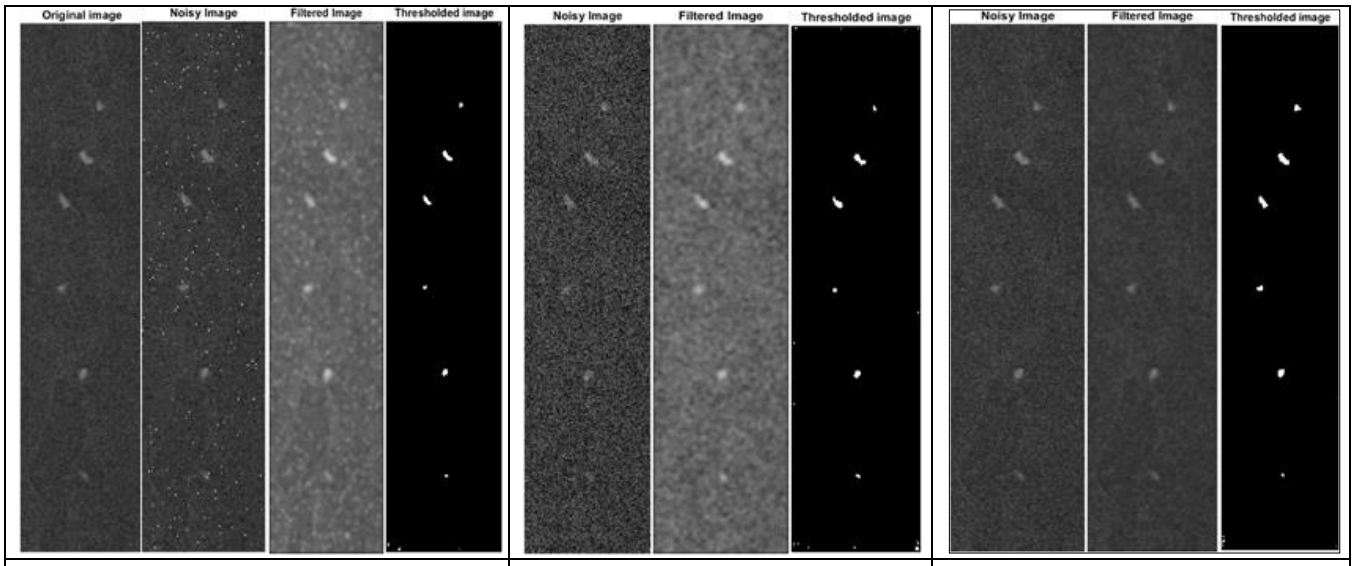

Salt and pepper Noise	Gaussian noise	Speckle noise

(b) PVAL

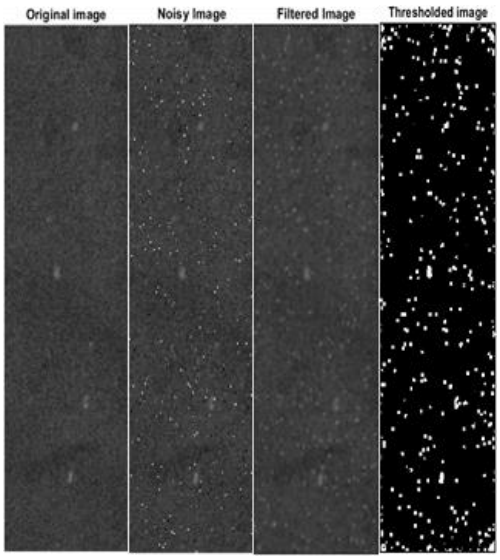	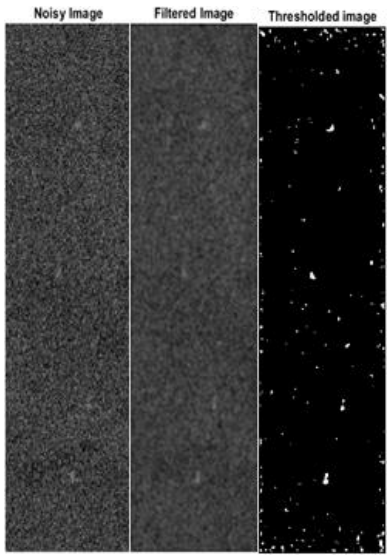	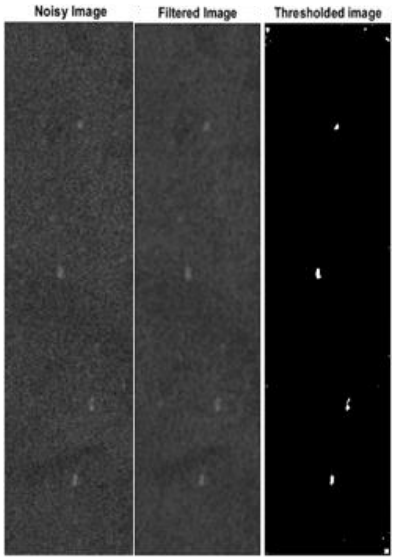
Salt and pepper noise	Gaussian noise	Speckle noise

(c) PVAL/G

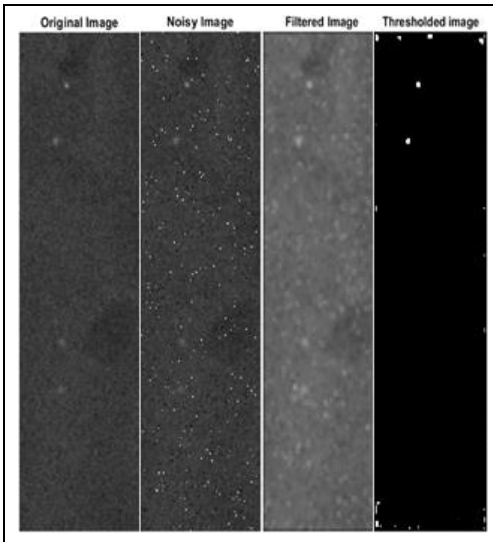	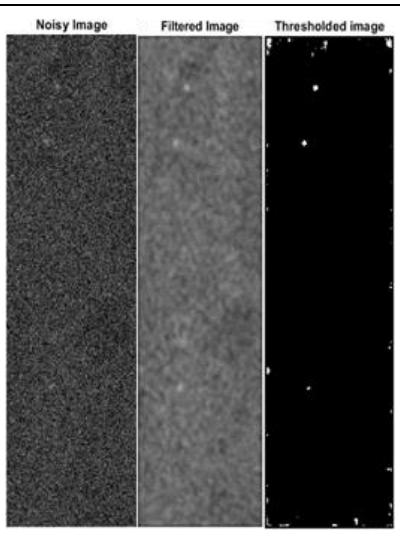	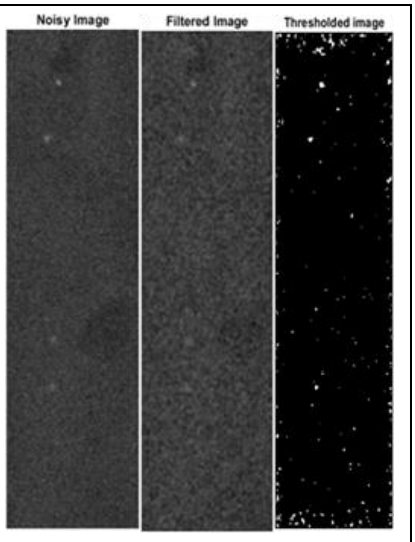
Salt and pepper noise	Gaussian noise	Speckle noise

(d) PVAL/H

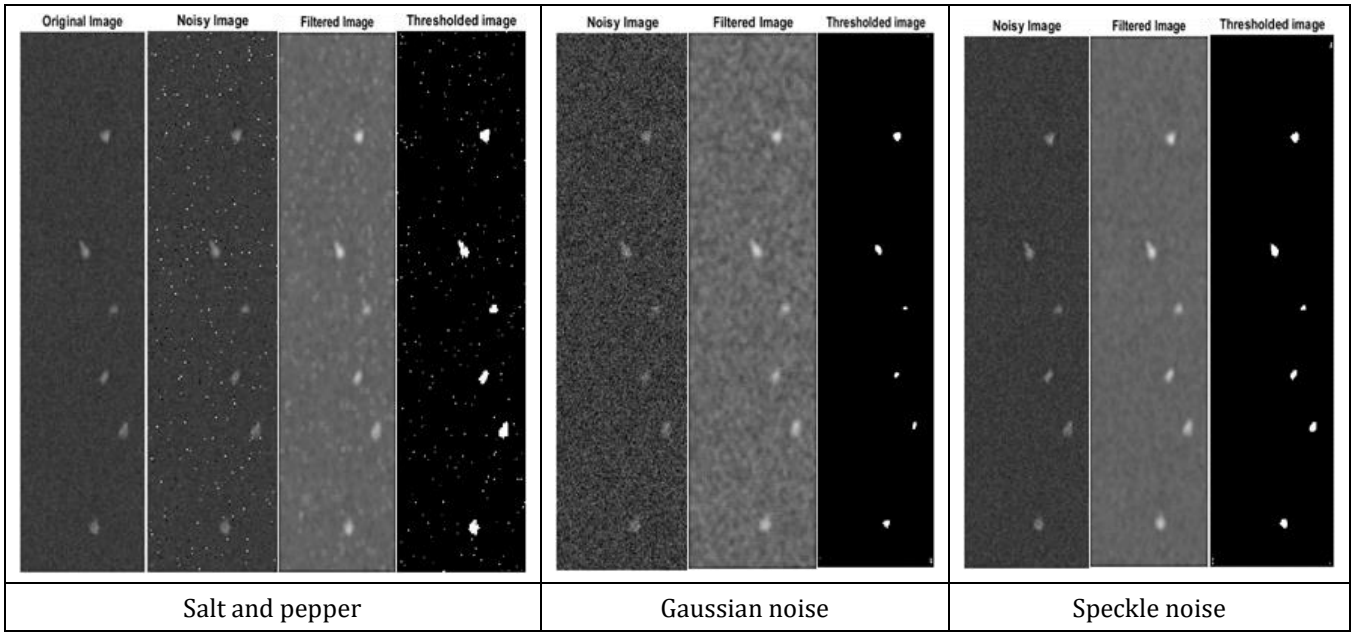

Figure 1 Enhanced images through the application of mean filter on (a) PVAL/E (b) PVAL (c) PVAL/G (d) PVAL/H

3.2. Median filter

Figure 2 (a) - (d) presents mammogram images of PVAL/E, PVAL, PVAL/G and PVAL/H preprocessed using median filter. The median filter performed poorly in the elimination of Gaussian noise compared to the salt & pepper and speckle noises. The performance of the median filter after denoising for salt & pepper is better than the mean filter. The quality of PVAL/G diminished with the application of the median filter.

(a) PVAL/E

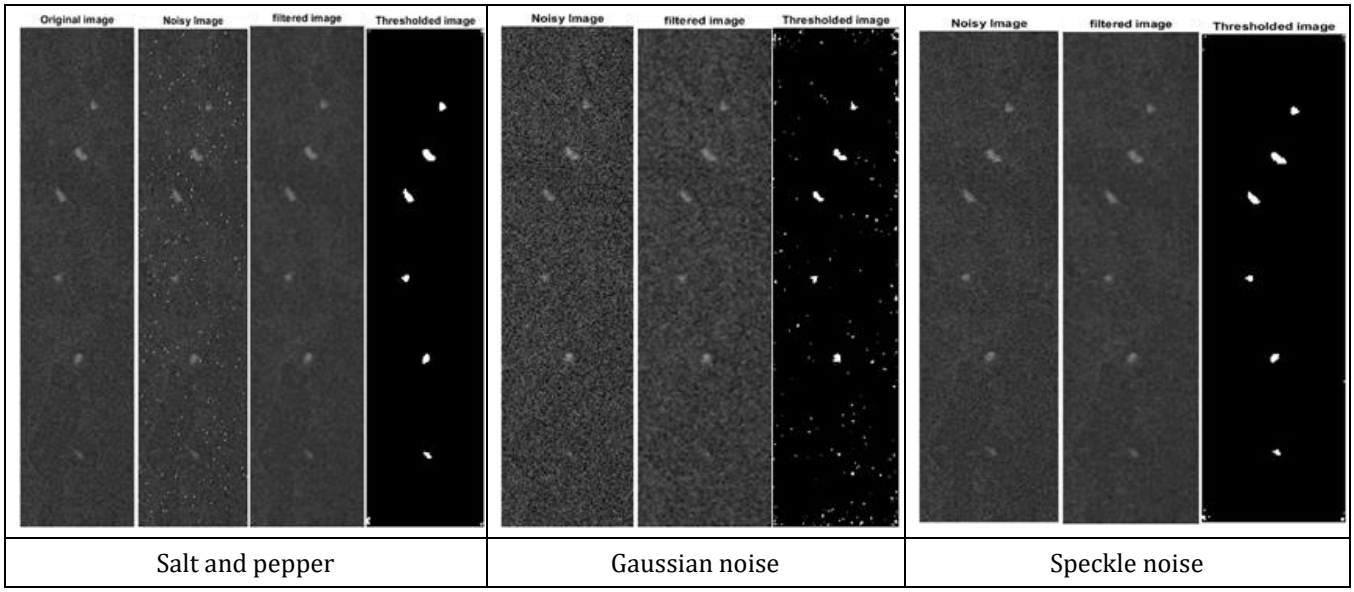

(b) PVAL

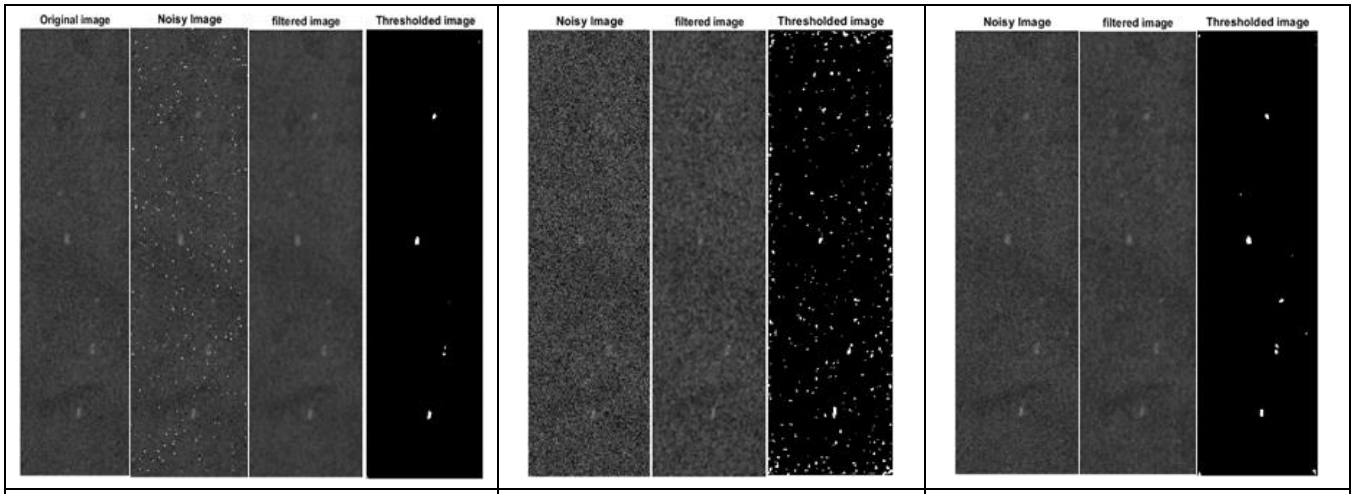

Salt & pepper noise	Gaussian noise	Speckle noise

(c) PVAL/G

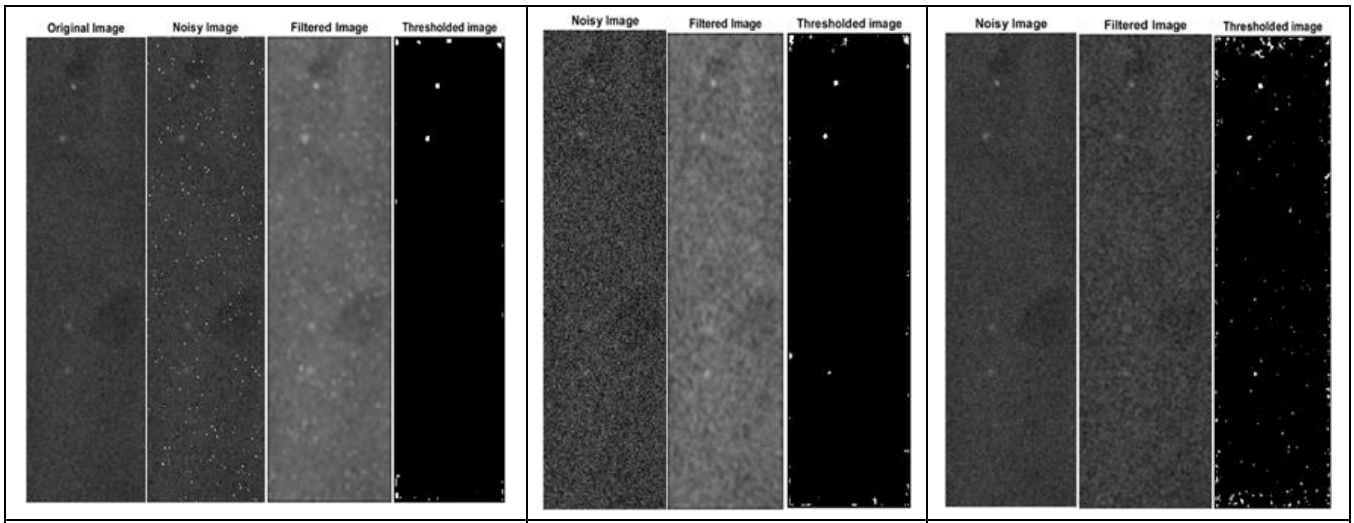

Salt & pepper noise	Gaussian noise	Speckle noise

(d) PVAL/H

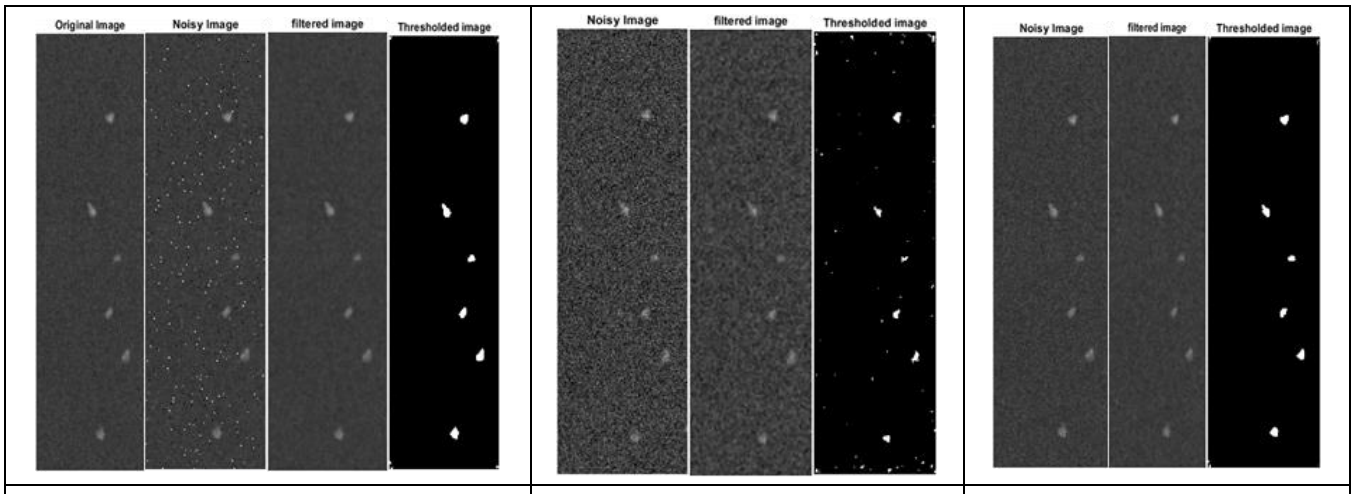

Salt & pepper noise	Gaussian noise	Speckle noise

Figure 2 Enhanced images through the application of median filter on (a) PVAL/E (b) PVAL (c) PVAL/G (d) PVAL/H

3.3. Gaussian filter

Figure 3 (a) - (d) presents mammogram images of PVAL/E, PVAL, PVAL/G and PVAL/H the quality of images obtained after denoising with Gaussian filter. The Gaussian filter recorded optimal performance in denoising images with all 3 types of added noise under consideration for PVAL/E and PVAL/H. This is because of the relatively lower density and higher contrast and CNR of the original images. This filter performed better than the mean and median filters.

(a) PVAL/E

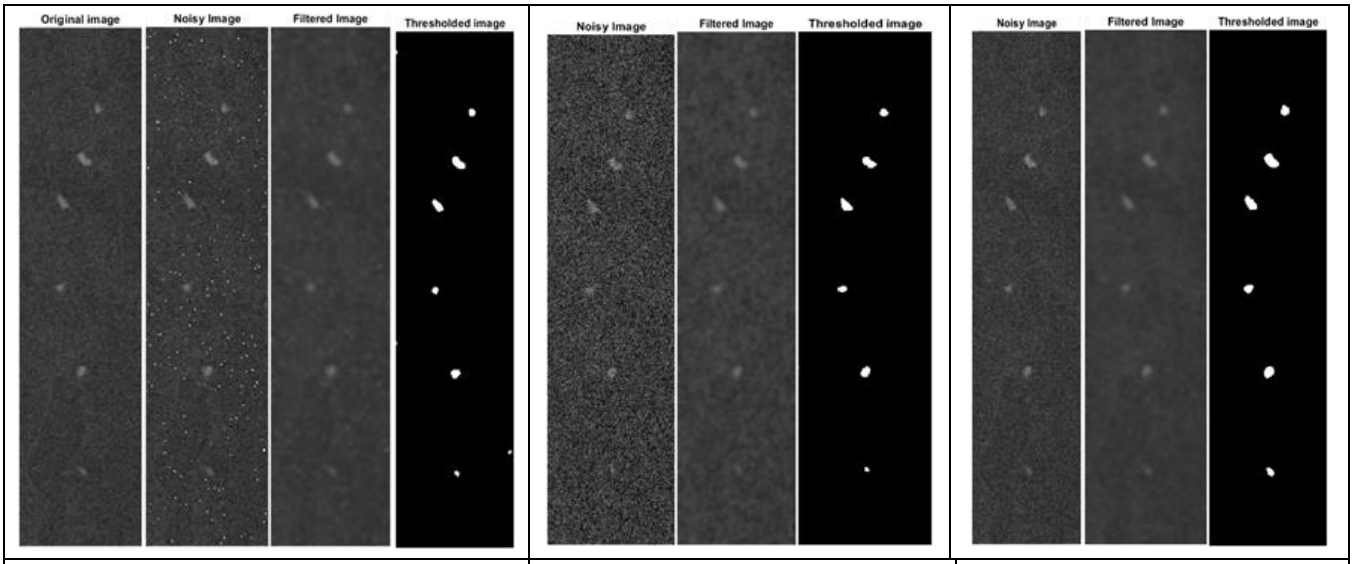

Salt & pepper noise	Gaussian noise	Speckle noise

(b) PVAL

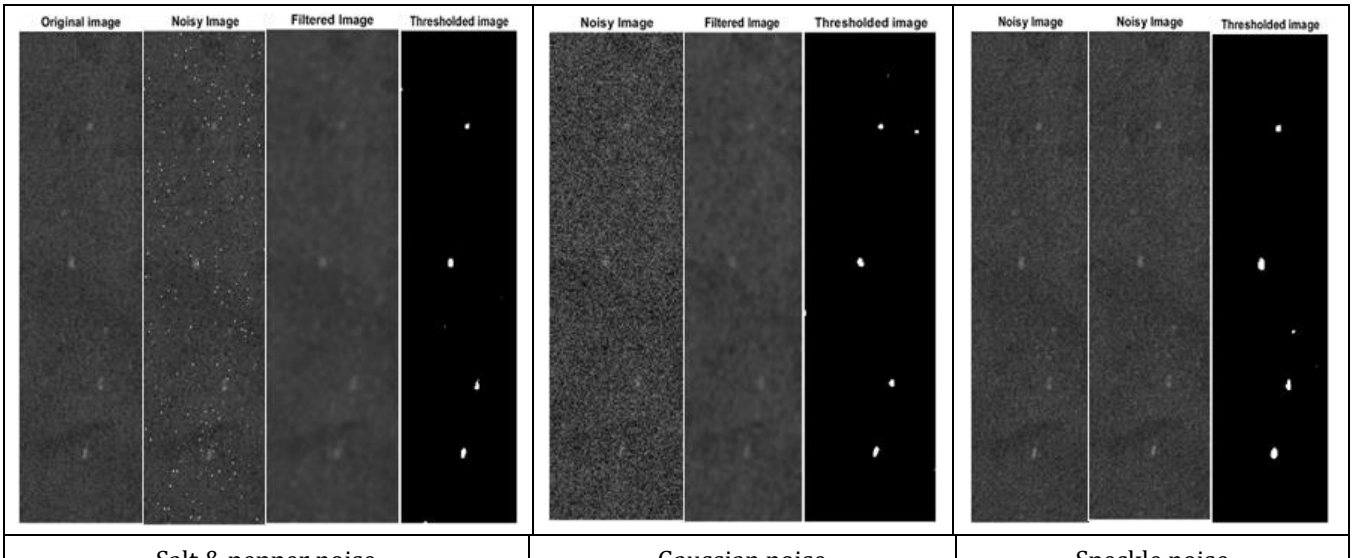

Salt & pepper noise	Gaussian noise	Speckle noise

(c) PVAL/G

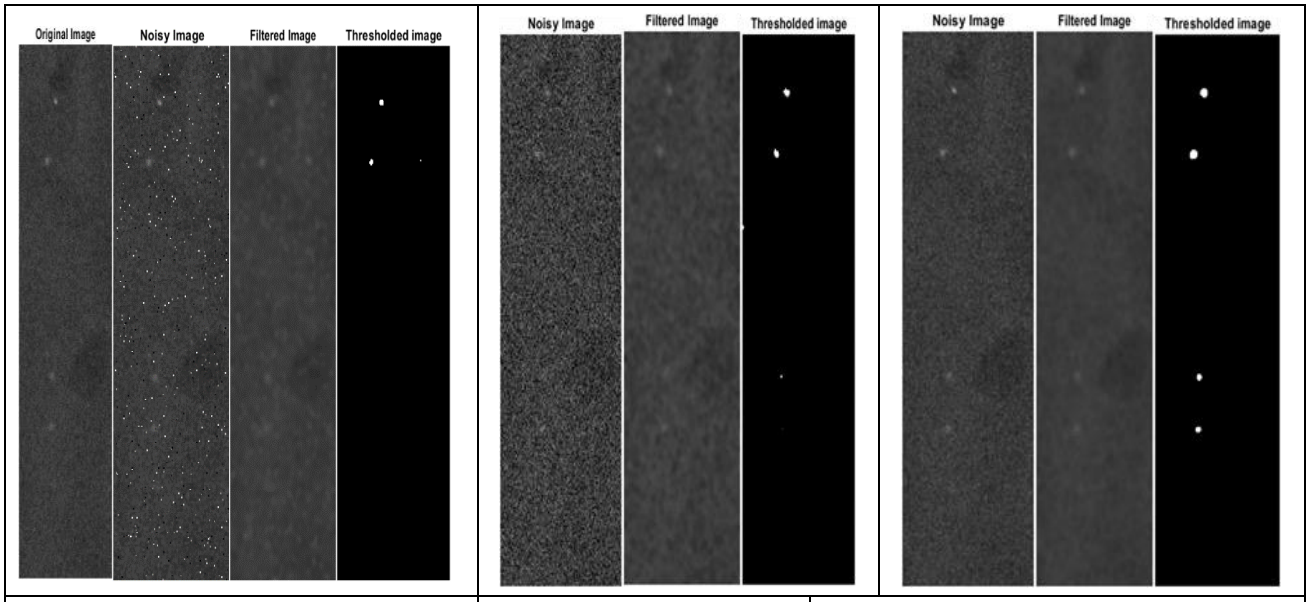

(d) PVAL/H

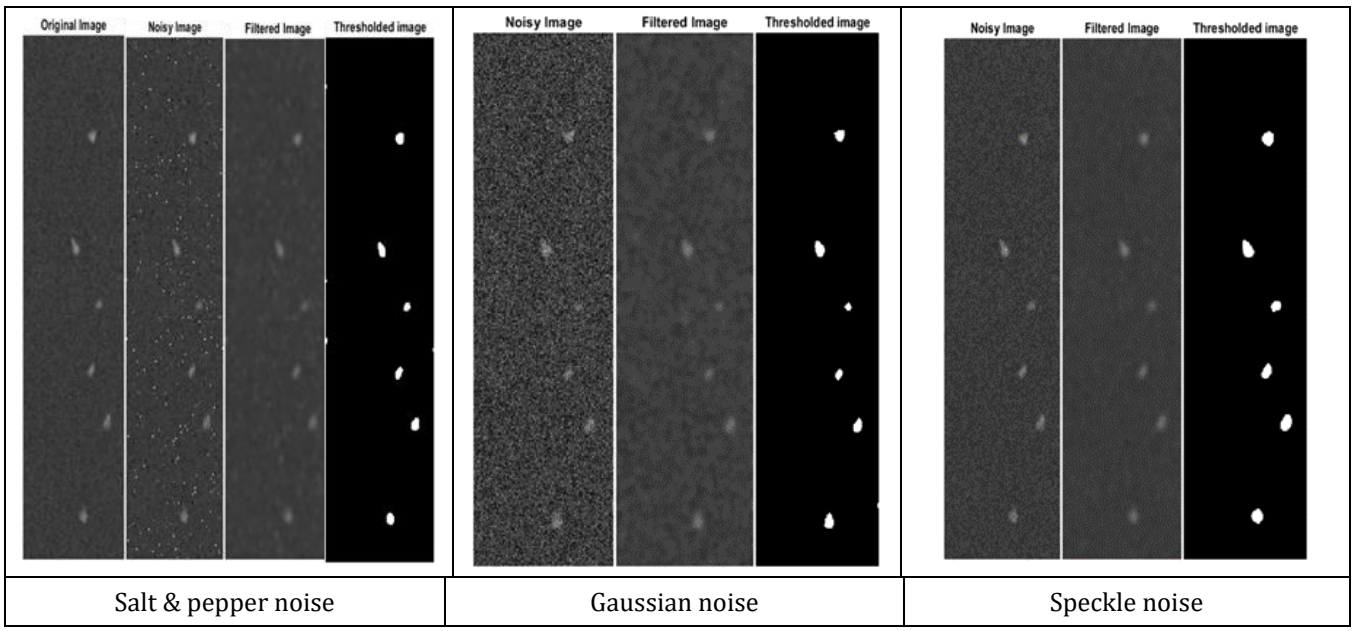

Figure 3 Enhanced images through the application of Gaussian filter on (a) PVAL/E (b) PVAL (c) PVAL/G (d) PVAL/H

3.4. Image quality metrics (IQM)

Tables 1, 2 and 3 show the results of calculated mean squared error (MSE), signal to noise ratio (SNR) and peak signal to noise ratio (PSNR) respectively. These IQM do not reflect perceptual image quality.

The MSE is one of the image quality parameters commonly employed to assess the quality of an image. Smaller values of MSE reflects better image quality. Table 1 presents the average MSE values of each tested filter. The median filter (salt & pepper and speckle noise) and mean filter (speckle noise) produced lower MSE values compared to the other filters used. The values of MSE achieved with the mean and median filters are consistent with previous studies that used similar filters to denoise mammogram images of the human breast (Joseph, John and Dhas, 2017; Kshema, George and Dhas, 2017). On the other hand, the mean filter performed poorly in denoising images with salt & pepper and Gaussian

noises. This was evident by high values of MSE ranging from 1617.1 to 2123.1 recorded by the mean filter. PVAL/H had the least MSE compared to the other phantoms. This was expected because of its high contrast value.

The signal to noise ratio (SNR) measures the sensitivity of an imaging system. Smaller values of SNR depict poor image quality. Table 2 shows the average SNR values of all filters employed. The result revealed that the median filter (for denoising salt & pepper and speckle noise) recorded the highest SNR values while mean filter (for denoising salt & pepper and Gaussian noise) recorded the least SNR.

Large values of PSNR indicate good image quality. Table 3 demonstrates the mean PSNR values of all tested filters. The results show that the mean filter did better in removing speckle noise compared to the salt & pepper and Gaussian noise (Figure 1, a – d). Though the Gaussian filter achieved good results for denoising all three types of added noises, the performance of Gaussian and median filter after denoising mammogram images with salt & pepper and speckle noises revealed the highest PSNR values compared to the mean filter. The results achieved in this work were in good agreement with past studies (Akila, Jayashree and Vasuki, 2015; Padmavathy *et al.*, 2018) The PSNR values for PVAL/H was superior to those of PVAL/E, PVAL and PVAL/G for all the filters tested. This result is consistent with the high contrast that characterize the original image of PVAL/H.

Table 1 Average MSE values of different pre-processing filters used

Image	**Mean filter**			**Median filter**			**Gaussian filter**		
	Salt & Noise	**Gaussian**	**Speckle**	**Salt & pepper**	**Gaussian**	**Speckle**	**Salt & pepper**	**Gaussian**	**Speckle**
PVAL/E	1617.1	1935.2	35.81	26.32	146.49	34.11	44.27	61.52	40.07
PVAL	1810.6	2123.1	39.27	28.42	147.06	37.38	47.72	61.43	41.62
PVAL/G	1680.6	1998.5	29.63	19.05	139.5	27.36	34.88	50.6	30.75
PVAL/H	1707.6	2038.8	21.9	9.92	131.2	19.17	24.96	42.02	19.7

Table 2 Average SNR values of different pre-processing filters used

Image	**Mean filter**			**Median filter**			**Gaussian filter**		
	Salt & Noise	**Gaussian**	**Speckle**	**Salt & pepper**	**Gaussian**	**Speckle**	**Salt & pepper**	**Gaussian**	**Speckle**
PVAL/E	7.72	7.25	19.79	21.15	14.17	19.98	18.98	17.87	19.32
PVAL	7.73	7.32	19.89	21.33	14.60	20.11	19.36	18.33	19.67
PVAL/G	7.75	7.29	20.79	22.74	14.55	21.13	20.22	18.86	20.66
PVAL/H	7.80	7.33	22.22	25.71	14.98	22.83	21.81	19.86	22.73

Table 3 Average PSNR values of different pre-processing filters used

Image	**Mean filter**			**Median filter**			**Gaussian filter**		
	Salt & Noise	**Gaussian**	**Speckle**	**Salt & pepper**	**Gaussian**	**Speckle**	**Salt & pepper**	**Gaussian**	**Speckle**
PVAL/E	16.04	15.26	32.59	33.92	26.47	32.81	31.67	30.24	30.41
PVAL	15.55	14.86	32.19	33.94	26.46	32.4	31.53	30.24	30.17
PVAL/G	15.88	15.12	33.4	35.33	26.29	33.76	32.7	31.08	31.69
PVAL/H	15.81	15.04	34.7	38.16	26.95	35.3	34.16	31.9	34.2

4. Conclusion

The basic noises usually present on mammogram images are salt and pepper noise, speckle noise and Gaussian noise. In this research, the performance of some denoising filters viz; mean, median, and Gaussian filters based on MSE, SNR, and PSNR show that the Gaussian filter outperformed the mean and median filters. The edges were better preserved, and the image smoothened with the Gaussian filter, thereby enhancing visibility of microcalcifications.

Compliance with ethical standards

Disclosure of conflict of interest

No conflict of interest to be disclosed.

References

[1] Akila, K., Jayashree, L. S. and Vasuki, A. (2015) 'Mammographic image enhancement using indirect contrast enhancement techniques - A comparative study', Procedia Computer Science, 47(C), pp. 255–261. doi: 10.1016/j.procs.2015.03.205.

[2] American College of Radiology (2013) ACR BIRADS Atlas - Mammography Reporting System. Available at: https://www.acr.org/-/media/ACR/Files/RADS/BI-RADS/Mammography-Reporting.pdf.

[3] Arvelos, J. M. et al. (2017) 'Development of breast phantom for quality assessment of mammographic images', in International Nuclear Atlantic Conference. Brazil.

[4] Dubey, R. B., Hanmandlu, M. and Gupta, S. K. (2010) 'A comparison of two methods for the segmentation of masses in the digital mammograms', Computerized Medical Imaging and Graphics, 34(3), pp. 185–191. doi: 10.1016/j.compmedimag.2009.09.002.

[5] Isa, I. S. et al. (2015) 'Evaluating denoising performances of fundamental filters for T2-weighted MRI images', Procedia Computer Science, 60(1), pp. 760–768. doi: 10.1016/j.procs.2015.08.231.

[6] Joseph, A. M., John, M. G. and Dhas, A. S. (2017) 'Mammogram image denoising filters: A comparative study', 2017 Conference on Emerging Devices and Smart Systems, ICEDSS 2017, (March), pp. 184–189. doi: 10.1109/ICEDSS.2017.8073679.

[7] Kabir, N. A., Okoh, F. O. and Mohd Yusof, M. F. (2021) 'Radiological and physical properties of tissue equivalent mammography phantom: Characterization and analysis methods', Radiation Physics and Chemistry, 180(June 2020), p. 109271. doi: 10.1016/j.radphyschem.2020.109271.

[8] Kshema, George, M. J. and Dhas, D. A. S. (2017) 'Preprocessing filters for mammogram images: A review', 2017 Conference on Emerging Devices and Smart Systems, ICEDSS 2017, (August 2018), pp. 1–7. doi: 10.1109/ICEDSS.2017.8073694.

[9] O'Grady, S. and Morgan, M. P. (2018) 'Microcalcifications in breast cancer: From pathophysiology to diagnosis and prognosis', Biochimica et Biophysica Acta - Reviews on Cancer, 1869(2), pp. 310–320. doi: 10.1016/j.bbcan.2018.04.006.

[10] Okoh, F. O. et al. (2022) 'Investigation of polyvinyl alcohol (PVAL) composite gels and the outcome of variation in breast phantom densities on image quality and dose in full-field digital mammography', Radiation Physics and Chemistry, 200(July), p. 110393. doi: 10.1016/j.radphyschem.2022.110393.

[11] Oliver, A. et al. (2012) 'Automatic microcalcification and cluster detection for digital and digitised mammograms', Knowledge-Based Systems, 28, pp. 68–75. doi: 10.1016/j.knosys.2011.11.021.

[12] Padmavathy, T. V. et al. (2018) 'Performance analysis of pre-cancerous mammographic image enhancement feature using non-subsampled shearlet transform', Multimedia Tools and Applications, pp. 1–16. doi: 10.1007/s11042-018-5951-3.

[13] Ponraj, D. and Jenifer, M. (2011) 'A Survey on the Preprocessing Techniques of Mammogram for the Detection of Breast Cancer', Journal of Emerging …, 2(12), pp. 656–664.

[14] Ramani, R., Vanitha, N. S. and Valarmathy, S. (2013) 'The Pre-Processing Techniques for Breast Cancer Detection in Mammography Images', International Journal of Image, Graphics and Signal Processing, 5(5), pp. 47–54. doi: 10.5815/ijigsp.2013.05.06.

[15] Zhang, Y. et al. (2012) 'An effective and objective criterion for evaluating the performance of denoising filters', Pattern Recognition, 45(7), pp. 2743–2757. doi: 10.1016/j.patcog.2012.01.015.